A Hamiltonian Boussinesq model with horizontally sheared currents

Elena Gagarina[1], Jaap van der Vegt, Vijaya Ambati, and Onno Bokhove[2]

Department of Applied Mathematics,
University of Twente, Enschede, Netherlands
[1]Email: e.gagarina@utwente.nl
[2]Email: o.bokhove@math.utwente.nl

Abstract

We are interested in the numerical modeling of wave-current interactions around beaches' surf zones. Any model to predict the onset of wave breaking at the breaker line needs to capture both the nonlinearity of the wave and its dispersion. We have formulated the Hamiltonian dynamics of a new water wave model. This model incorporates both the shallow water model and the potential flow model as limiting systems. The variational model derived by Cotter and Bokhove (2010) is such a model, but the variables used have been difficult to work with. Our new model has a three–dimensional velocity field consisting of the full three–dimensional potential field plus horizontal velocity components, such that the vertical component of vorticity is nonzero. Our aims are to augment the new model locally with bores and to derive a numerical finite element discretization of the new model including the capturing of bores. As a preliminary step, the variational finite element discretization of Miles' variational principle coupled to an elliptic mesh generator is shown.

1. Introduction

The beach surf zone is defined as the region of wave breaking and white capping between the moving shore line and the (generally time-dependent) breaker line. Consider nonlinear waves in the deeper water outside the surf zone approaching the beach, before any significant wave breaking occurs. The start of the surf zone on the offshore side is at the breaker line at which sustained wave breaking begins. It demarcates the points where the nonlinearity of the waves becomes strong enough to outweigh dispersion. The waves thus start to overturn. A mathematical model that can predict the onset of wave breaking at the breaker line will need to capture the nonlinearity of the wave and its dispersion.

Various mathematical models are used to simulate water waves. Smooth waves in the deep-water regions can be described by the potential flow model from which vorticity is absent. In the near-shore region, vorticity effects are important. When obliquely incident waves shoal in shallow water, steepen and break, a horizontal shear or a vertical vorticity is generated. On semi-enclosed or enclosed beaches, this leads to an overall circulation induced by wave breaking. A classical hydraulic model for the surf zone is the shallow water model. Breaking waves are approximated in this model by discontinuities with special relations holding across the jumps — the so-called bores, representing the complicated, turbulent three-dimensional wave breaking. Shallow water waves are not dispersive, and these waves tend to break too early in comparison with the real phenomena. Boussinesq models include internal wave dispersion to a higher degree of accuracy, but dispersion always seems to beat

nonlinearity. Therefore wave overturning tends to be prevented in these models. The variational Boussinesq model proposed by Klopman et al. (2010) may be a notable exception, but it is based on the Ansatz of potential flow. In three dimensions, a potential flow model cannot be extended by inclusion of bores and hydraulic jumps as a simple model to represent wave breaking. The reason is that at least some vorticity has to be generated by bores that have non-uniformities along their jump line (Peregrine 1998, Peregrine and Bokhove 1998). We therefore seek to develop a more advanced model that minimally captures both the shallow water approximation of breaking waves as bores and the accurate dispersion of the potential flow model.

2. New water wave model

2.1 Variational principle

Consider an incompressible fluid at time t in a three-dimensional domain bounded by walls and a free surface with horizontal coordinates $\bar{x}$, and vertical coordinate y. The water depth is denoted by $h = h(\bar{x}, t)$. There exists a parent Eulerian variational principle for incompressible flow with a free surface. Its velocity field contains both potential and rotational parts and is represented as $\bar{U}(\bar{x}, y, t) = \nabla\phi(\bar{x}, y, t) + (\nabla\bar{l}(\bar{x}, y, t))^T \bar{\pi}(\bar{x}, y, t)$ through Clebsch variables: the velocity potential ϕ, three-dimensional fluid parcel label $\bar{l}$ and corresponding Lagrange multiplier vector $\bar{\pi}$.

Cotter and Bokhove (2010) derived novel water wave dynamics from this parent variational principle constructed to include two limits: Luke's variational principle giving the classical potential water wave model and a principle for depth-averaged shallow water flows based on planar Clebsch variables. Shallow water flows only contain the vertical component of the vorticity $\nabla \times \bar{U}$ and depend only on horizontal coordinates and time. At least conceptually, the novel variational principle follows readily from the parent principle with two-dimensional label and multiplier fields $\bar{l}$ and $\bar{\pi}$ depending only on the two-dimensional horizontal components and time. Hence, they no longer depend on the vertical coordinate y.

Here we reduce the model to a more compact and conventional form. This reduction from six Clebsch variables $\{\phi, h, \bar{l}, \bar{\pi}\}$ to four more conventional variables $\{\phi, h, \bar{u}^*\}$ is undertaken in a Hamiltonian setting. The latter variables involve a new velocity $\bar{u}^*$: the horizontal velocity evaluated at the free surface.

The resulting principle of Cotter and Bokhove (2010) has the following form:

$$0 = \delta \int_0^T L[\bar{l}, \bar{\pi}, \phi, h]\, dt = \delta \int_0^T \int_\Omega \partial_t \phi + \frac{1}{2}\left|\nabla\phi + \bar{\mathrm{v}}\right|^2 d\bar{x}\, dy + \int_{\partial\Omega_S} h\bar{\pi} \cdot \partial_t \bar{l} + \frac{1}{2} g((h+b)^2 - b^2)\, d\bar{x}\, dt$$

$$= \delta \int_0^T \int_\Omega \partial_t \phi + \bar{\pi} \cdot \partial_t \bar{l}\, d\bar{x} dy + H dt\,, \qquad (1)$$

where g is the constant acceleration of the Earth's gravity, $\bar{\mathrm{v}} = (\nabla\bar{l}(\bar{x}, t))^T \bar{\pi}(\bar{x}, t)$ such that $\bar{U}(\bar{x}, y, t) = \nabla\phi(\bar{x}, y, t) + \bar{\mathrm{v}}(\bar{x}, t)$, and the time-dependent fluid domain Ω with a free surface boundary $\partial\Omega_S$ is given by $y = h(\bar{x}, t) + b(\bar{x})$, where $h(\bar{x}, t)$ is the water depth and $b(\bar{x})$ a given, fixed topography. The Hamiltonian is the sum of kinetic and potential energies

$$H = H[\bar{l}, \bar{\pi}, \phi, h] = \int_{\Omega} \frac{1}{2} \left| \nabla \phi + \bar{\mathrm{v}} \right|^2 \, d\bar{x}\, dy + \int_{\partial\Omega_s} \frac{1}{2} g((h+b)^2 - b^2)\, d\bar{x} \,. \tag{2}$$

With suitable boundary conditions, the dynamics follows from (1) and (2) as

$$\begin{aligned}
&\delta\phi: \quad \nabla^2 \phi + \nabla \cdot \bar{\mathrm{v}} = 0 \,, \\
&\delta h: \quad \partial_t \phi_s + \frac{1}{2} \left| \nabla_{\bar{x}} \phi_s + \bar{\mathrm{v}} \right|^2 + g(h+b) - \bar{\mathrm{v}} \cdot \bar{u} - \frac{1}{2} (\partial_y \phi)_s^2 (1 + (\nabla_{\bar{x}} (h+b))^2) = 0 \,, \\
&\delta \phi_s: \quad (\partial_y \phi)_s (1 + (\nabla_{\bar{x}} (h+b))^2) - (\nabla_{\bar{x}} \phi_s + \bar{\mathrm{v}}) \nabla_{\bar{x}} (h+b) - \partial_t h = 0 \,, \\
&\delta(h\bar{\pi}): \quad \partial_t \bar{l} + \bar{u} \cdot \nabla \bar{l} = 0 \,, \\
&\delta \bar{l}: \quad \partial_t (h\bar{\pi}) + \nabla \cdot (h \bar{u} \bar{\pi}) = 0 \,,
\end{aligned} \tag{3}$$

with the depth-weighted horizontal velocity vector

$$h\bar{u}(\bar{x}, t) = \int_b^{b+h} \bar{U}_H dy \,, \tag{4}$$

and surface velocity potential $\phi_s = \phi_s(\bar{x}, t) = \phi(\bar{x}, y = h + b, t)$. Subscript $(.)_H$ denotes the horizontal component of the vector. System (3) is a slight variation of the one derived in Cotter and Bokhove (2010) in that it yields the canonical formulation described next in section 2.2.

2.2 Hamiltonian dynamics

System (3) rewritten in Hamiltonian form readily becomes

$$\begin{aligned}
&\delta\phi: \quad \nabla^2 \phi + \nabla \cdot \bar{\mathrm{v}} = 0 \,, \\
&\delta h: \quad \partial_t \phi_s = -\frac{\delta H}{\delta h} \,, \quad \delta \phi_s: \quad \partial_t h = \frac{\delta H}{\delta \phi_s} \,, \\
&\delta(h\bar{\pi}): \quad \partial_t \bar{l} = -\frac{\delta H}{\delta (h\bar{\pi})} \,, \quad \delta \bar{l}: \quad \partial_t (h\bar{\pi}) = \frac{\delta H}{\delta \bar{l}} \,.
\end{aligned} \tag{5}$$

The form of equations in (5) is similar to that of Hamiltonian classical mechanics. The pairs $\{h, h\bar{\pi}\}$ and $\{\phi_S, \bar{l}\}$ of variables at the free surface are canonically conjugated. Thus the Hamiltonian dynamics arising from (5) is canonical and takes the form

$$\frac{dF}{dt} = \iint \frac{\delta F}{\delta h} \frac{\delta H}{\delta \phi_s} - \frac{\delta F}{\delta \phi_s} \frac{\delta H}{\delta h} + \frac{\delta F}{\delta (h\bar{\pi})} \cdot \frac{\delta H}{\delta \bar{l}} - \frac{\delta F}{\delta \bar{l}} \cdot \frac{\delta H}{\delta (h\bar{\pi})} d\bar{x} \,. \tag{6}$$

Substitution of one of the variables $h, h\bar{\pi}, \phi_s, \bar{l}$ rewritten as functional, in a particularization of the functional F, yields the equation for this variable.

Our next step is to reduce the number of variables by moving from the set $\left\{\phi, h, \phi_s, \bar{l}, h\bar{\pi}\right\}$ to the set $\left\{\phi, h, \phi_s, \bar{u}^*\right\}$. Doing so removes the reference to the label fields and their conjugates in a reduction to one surface velocity field. This transformation is achieved via variational techniques. The surface velocity is defined as $\bar{u}^*(\bar{x}, t) = \nabla \phi_S(\bar{x}, t) + \bar{\mathrm{v}}(\bar{x}, t)$, while the potential vorticity is $q = (\partial_{x_1} \bar{\mathrm{v}}_2 - \partial_{x_2} \bar{\mathrm{v}}_1) / h = (\partial_{x_1} \bar{u}_2^* - \partial_{x_2} \bar{u}_1^*) / h$. The resulting Hamiltonian dynamics has the form

$$\frac{dF}{dt} = \iint -q \frac{\delta F}{\delta \bar{u}^*} \cdot \frac{\delta H}{\delta \bar{u}^*}^{\perp} - \frac{\delta F}{\delta h} \nabla \cdot \frac{\delta H}{\delta \bar{u}^*} + \frac{\delta H}{\delta h} \nabla \cdot \frac{\delta F}{\delta \bar{u}^*} d\bar{x}\,, \tag{7}$$

where the Hamiltonian is

$$H = H[\phi, h, \phi_S, \bar{u}^*] = \int_\Omega \frac{1}{2} \left| \bar{u}^* + \nabla(\phi - \phi_s) \right|^2 d\bar{x}\, dy + \int_{\partial\Omega_S} \frac{1}{2} g((h+b)^2 - b^2)\, d\bar{x}\,, \tag{8}$$

and the vector $\left(\delta H / \delta \bar{u}^*\right)^{\perp}$ is obtained from vector $\delta H / \delta \bar{u}^*$ turned by 90° counterclockwise. One can notice that the bracket (7) is in essence the same as the shallow water bracket derived in, e.g., Salmon (1988).

The final system of equations in new variables is as follows

$$\partial_t h + \nabla \cdot (h\bar{u}) = 0\,, \tag{9}$$

$$\partial_t \bar{u}^* + \nabla B + q(h\bar{u})^{\perp} = 0\,,$$

with constraints

$$\nabla \cdot \bar{u}^* + \nabla^2(\phi - \phi_s) = 0 \tag{10}$$

and

$$\nabla \cdot \bar{u}^* = \nabla^2 \phi_s\,. \tag{11}$$

where the depth-weighted horizontal velocity vector in (4) can be redefined as

$$h\bar{u}(\bar{x}, t) = \int_b^{b+h} (\bar{u}^* + \nabla_H(\phi - \phi_s)) dy\,. \tag{12}$$

and the Bernoulli function takes the form

$$B = \frac{1}{2} \left| \bar{u}^* \right|^2 + g(h+b) - \frac{1}{2} (\partial_y \phi)_s^2 (1 + (\nabla(h+b))^2) = 0\,. \tag{13}$$

The required boundary condition at the shore line is $h = 0$, and at a solid wall $\bar{n} \cdot h\bar{u} = 0$.

3. Limiting systems

It was our goal to derive a water wave model incorporating the relevant properties of both the shallow water model and the potential flow model. These two models are the limiting systems of the new water wave model, as we show next. The new water wave model reduces to the water wave equations under potential flow when we take $\bar{U} = \nabla\varphi$. The shallow water limit is reached when we restrict $\phi = \phi(\bar{x}, y, t)$ to the surface potential $\phi_s = \phi_s(\bar{x}, t)$ under the extension to Luke's variational principle. Then the second equation in (9) will be transformed to the depth-averaged shallow water momentum equation $\partial_t \bar{u}^* + \bar{u}^* \cdot \nabla \bar{u}^* + g\nabla(h+b) = 0$.

Klopman et al (2010) presented a Boussinesq methodology in which the vertical structure of the fluid motion beneath the free surface is approximated. Klopman sketched how to add the vorticity term to the potential flow models afterwards. In contrast, we include the vorticity systematically from the onset. The Hamiltonian structure, postulated in Klopman et al (2010) for a restricted potential flow approximation in the vertical, is here derived cleanly for all three-dimensional potential flow components plus a generic horizontal velocity field at the free surface. Under the assumption of a vertical structure of the velocity potential our new water wave model results into a system equivalent to the Boussinesq-like model proposed by Klopman.

4. Galerkin finite element discretization

4.1 Potential flow

The potential flow model is the classical model for dispersive water waves. It is based on the assumption that the three-dimensional velocity $\bar{U}$ depends solely on the gradient of a velocity potential ϕ, such that $\bar{U} = \nabla\phi$. Luke (1967) and Miles (1977) each derived the water wave model from closely related and interchangeable variational principles. The new water wave model of Cotter and Bokhove (2010) was derived from an extension of Luke's variational principle. Therefore, the verification of the numerical method on the potential flow model is a vital, first step.

A new space continuous and time discontinuous Galerkin finite element discretization of Miles' variational principle was developed by Ambati et al. (2012). A straightforward Galerkin finite element expansion was simply substituted in the variational principle, in which the mesh movement was designed to be an integral part of the dynamics. A time discontinuous finite element expansion was used to harness the complexity of combined horizontal and vertical node movement in the neighborhood of the moving wave maker. This resulted in a stable, conservative method — even for high-frequency motions of the wave maker. The model was verified to be second order in both space and time, and successfully validated against wave tank data obtained from the Maritime Institute of The Netherlands.

Our future aims are to extend this numerical model to incorporate a discretization of Luke's variational principle and our new formulations (1) or (7). Consequently, more versatile nodal movement in the interior and at the free surface is required because — unlike in Miles' model — the free surface can (locally) become multivalued in a bore. Here we test a selected elliptic mesh generator coupled to Miles' variational principle.

4.2 Numerical model

Miles' variational principle is explored firstly in a vertical plane. We consider finite elements in two dimensions. The domain $\Omega \subset R^2$ is partitioned into a mixture of N_{el} quadrilateral or triangular elements such that we obtain the tessellation

$$T_h = \left\{ K_k \,|\, \bigcup_{k=1}^{N_{el}} \bar{K}_k = \bar{\Omega}; \quad K_k \cap K_{k'} = \varnothing \quad if \quad k \neq k', 1 \leq k, k' \leq N_{el} \right\}, \tag{14}$$

with $\bar{K}_k$ the closure of element K_k. We introduce a reference element $\hat{K}$ with a local coordinate system (ξ, η) and define the mapping $F_k: \ \hat{K} \rightarrow K_k$ between the reference element $\hat{K}$ and element K_k as follows

$$x = F_k(\xi,\eta) = \sum_\gamma x_\gamma \varphi_\gamma(\xi,\eta) \quad \text{and} \quad z = F_k(\xi,\eta) = \sum_\gamma z_\gamma \varphi_\gamma(\xi,\eta), \tag{15}$$

with (x_γ, z_γ) the position of the local nodes and φ_γ the mapping, for $\gamma = 1,..., N_p$. For triangles with straight edges $N_p = 3$ the mappings are $\varphi_1 = 1 - \xi - \eta, \varphi_2 = \xi, \varphi_3 = \eta$; and for quadrilaterals with straight edges $N_p = 4$ the mappings are $\varphi_\gamma = (1 \pm \xi)(1 \pm \eta)/4$. The mappings also play the role of basis functions in the Galerkin method when a linear polynomial expansion is used. A Galerkin expansion will be used to approximate the

variables as well as the given topography function b. The variables expanded in this way are denoted via a subscript that denotes the mesh size $\hbar$, e.g., $h \to h_\hbar$. Either quadrilateral or triangular elements are used, or a mixture of the two. On the free surface one-dimensional Galerkin expansions with basis functions ψ_l will be used for ϕ_s, h and b.

The Galerkin finite element Miles' variational principle becomes

$$0 = \int_0^T \int_0^L \phi_{s\hbar} \partial_t h_\hbar - \frac{1}{2} g((h_\hbar + b_\hbar)^2 - b_\hbar^2)\, dx - \int_{b_\hbar}^{b_\hbar + h_\hbar} \frac{1}{2} |\nabla \phi_\hbar|^2 \, dx\, dy\, dt \,. \tag{16}$$

The Galerkin expansions are $\phi_\hbar(x,y,t) = \sum_i \phi_i(t) \varphi_i(x,y,t)$, $h_\hbar(x_1,y,t) = \sum_l h_l(t) \psi_l(x)$, $\phi_{s\hbar}(x,y,t) = \sum_l \phi_l(t) \psi_l(x)$ and $b_\hbar(x,y,t) = \sum_l b_l(t) \psi_l(x)$ for $l = 1,...,N_x$ and $i = 1,...,N_n$.

Substitution of expansions into (16) yields the finite element variational principle. Basis functions φ_i for elements bordering a free surface boundary coincide with the relevant basis function ψ_l at that surface boundary. The nodes are lined up such that the first $k, l = 1,..., N_x$ nodes lie at the free surface. All nodes have indices $i, j = 1,..., N_n$ and the interior nodes are denoted by $i', j' = N_x + 1,..., N_n$.

At first, we let the interior nodes move in the vertical only such that each node resides at a fixed fraction of the time dependent total depth h_k at horizontal position x_k. Consequently, the basis function $\varphi_i(x,y,t)$ for the velocity potential is time dependent. For example, for a regular discretization in the vertical with N_y nodes spaced $\Delta z_k = h_k / (N_y - 1)$ apart, each node is placed at $z_{kj} = b_k + (N_y - j) h_k / (N_y - 1)$ with $j = 1,..., N_y$.

After substitution of the above Galerkin expansions into (16), the discrete variational principle and its variations become

$$0 = \delta \int_0^T M_{kl} \left(\phi_l \dot{h}_k - \frac{1}{2} g (h_k + b_k)(h_l + b_l) + \frac{1}{2} g b_k b_l \right) + \frac{1}{2} A_{ij}(h_k) \phi_i \phi_j dt \tag{17}$$

$$= \int_0^T \left(M_{kl} \dot{h}_k - A_{il} \phi_l \right) \delta \phi_l - \left(M_{kl} \left(\dot{\phi}_l + g(h_l + b_l) \right) + C_{kij} \phi_i \phi_j \right) \delta h_k + A_{ij'} \phi_i \, \delta \phi_{j'} \, dt \,,$$

with matrix $M_{kl} = \int_0^L \psi_k \psi_l \, dx$ dx defined using free surface basis functions, and matrices

$$A_{ij} = \frac{1}{2} \int_0^L \int_{b_\hbar}^{b_\hbar + h_\hbar} \nabla \varphi_i \nabla \varphi_j \, dx dy \quad \text{and} \quad C_{kij} = \frac{\partial A_{ij}}{\partial z_m} \frac{\partial z_m}{\partial h_k}, \tag{18}$$

where we used a mapping from the local node number γ in element K to the relevant surface node $k_\gamma = k_\gamma^K$. For a regular rectangular mesh topology, this mapping is easily identified. The time derivative is denoted by dot: $\dot{h}_k = \frac{dh_k}{dt}$. To evaluate (18), we use

$$\delta A_{\alpha\beta} = \frac{1}{2} \delta \iint \frac{1}{|J|} \begin{pmatrix} z_\eta \partial_\xi \varphi_\alpha - z_\xi \partial_\eta \varphi_\alpha \\ -x_\eta \partial_\xi \varphi_\alpha + x_\xi \partial_\eta \varphi_\alpha \end{pmatrix} \cdot \begin{pmatrix} z_\eta \partial_\xi \varphi_\beta - z_\xi \partial_\eta \varphi_\beta \\ -x_\eta \partial_\xi \varphi_\beta + x_\xi \partial_\eta \varphi_\beta \end{pmatrix} d\xi \, d\eta \tag{19}$$

$$= \frac{1}{2}\iint \frac{1}{|J|}\Big(\big(z_\eta \partial_\xi \varphi_\beta - z_\xi \partial_\eta \varphi_\beta\big)\big(\partial_\xi \varphi_\alpha \delta z_\eta - \partial_\eta \varphi_\alpha \delta z_\xi\big) + \big(z_\eta \partial_\xi \varphi_\alpha - z_\xi \partial_\eta \varphi_\alpha\big)\big(\partial_\xi \varphi_\beta \delta z_\eta - \partial_\eta \varphi_\beta \delta z_\xi\big)$$

$$+\big(-x_\eta \partial_\xi \varphi_\beta + x_\xi \partial_\eta \varphi_\beta\big)\big(-\partial_\xi \varphi_\alpha \delta x_\eta + \partial_\eta \varphi_\alpha \delta x_\xi\big) + \big(-x_\eta \partial_\xi \varphi_\alpha + x_\xi \partial_\eta \varphi_\alpha\big)\big(-\partial_\xi \varphi_\beta \delta x_\eta + \partial_\eta \varphi_\beta \delta x_\xi\big)\Big)$$

$$+\frac{1}{|J|^2}\Big(\big(z_\eta \partial_\xi \varphi_\alpha - z_\xi \partial_\eta \varphi_\alpha\big)\big(z_\eta \partial_\xi \varphi_\beta - z_\xi \partial_\eta \varphi_\beta\big)$$

$$+\big(-x_\eta \partial_\xi \varphi_\alpha + x_\xi \partial_\eta \varphi_\alpha\big)\big(-x_\eta \partial_\xi \varphi_\beta + x_\xi \partial_\eta \varphi_\beta\big)\Big)\big(x_\eta \delta z_\xi - x_\xi \delta z_\eta + z_\xi \delta x_\eta - z_\eta \delta x_\xi\big) d\xi\, d\eta\,,$$

with the determinant of the Jacobian defined as $|J| = z_\eta x_\xi - x_\eta z_\xi$.

The resulting system of ordinary equations follows from (17) as

$$\begin{aligned} \delta\phi_l: &\quad M_{kl}\dot{h}_k - A_{il}(h_m)\phi_i = 0\,, \\ \delta h_k: &\quad M_{kl}\left(\dot{\phi}_l + g(b_l + h_l)\right) + C_{kij}(h_m)\phi_i\phi_j = 0\,, \\ \delta\phi_{j'}: &\quad A_{i'j'}(h_m)\phi_{i'} + A_{lj'}(h_m)\phi_l = 0\,. \end{aligned} \tag{20}$$

The symplectic Stormer Verlet scheme is used for the time discretization.

The method has been used for modeling standing waves, Fenton-Rienecker waves and waves generated by a wavemaker. The Maritime Institute of The Netherlands (MARIN) provided the wave tank data. A piston type wave maker is placed at the left side of the domain. The configuration is set up such that highly irregular waves are generated. For all the test cases, the numerical measurements were found to agree well with the experimental measurements (Ambati et al, 2012).

4.3 Mesh movement

The next step is to implement Luke's variational principle (Luke, 1967). Its formulation allows the free surface to be multivalued. Therefore, the vertical node connection used above is no longer valid. The new node connection should ensure that the variation of the free surface coordinates induces the variation of interior coordinates. One of the most widely used methods of grid generation is to determine coordinates (x, y) as a solution of a system of elliptic equations with Dirichlet boundary conditions, such as in Knupp (1992).

Before fully implementing Luke's variational principle coupled with Knupp' mesh movement, we introduce the mesh movement in the existing nonlinear potential flow code based on Miles' variational principle. Firstly, that allows testing of the numerical algorithm; secondly this generates the potential flow code under adaptive mesh movement.

In Knupp (1992) a variational principle is proposed that results in a robust automatic elliptic grid generator. It means that a generated grid will unfold and "automatic" means that no arbitrary parameters are required. The area-orthogonal grid generator often gives smooth, near-orthogonal and near-equal area meshes. The grid generator is expressed in terms of mappings $x = x(\xi,\eta),\quad y = y(\xi,\eta)$ from the logical space $\{(\xi,\eta) \in [0,1]\times[0,1]\}$ to the physical domain defined by its boundaries. The system of equations is

$$\begin{aligned} &g_{22}x_{\xi\xi} + 4x_\xi x_\eta x_{\xi\eta} + g_{11}x_{\eta\eta} + 2(x_\xi y_\eta + y_\xi x_\eta)y_\eta = 0\,, \\ &g_{22}y_{\xi\xi} + 4y_\xi y_\eta y_{\xi\eta} + g_{11}y_{\eta\eta} + 2(x_\xi y_\eta + y_\xi x_\eta)x_\eta = 0\,. \end{aligned} \tag{21}$$

The mesh movement algorithm allows to deal with steep wave profiles as shown in Fig. 1.

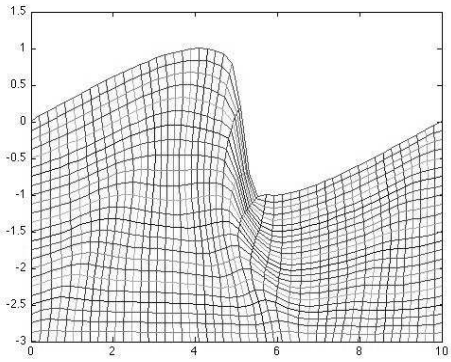

Figure 1: Adaptive mesh movement tested on a free surface using Burgers' equation to define an overturning "free surface".

System (17) variationally coupled with system (21) was tested against the standing waves case. Various wave profiles and corresponding grids are shown below at Fig. 2.

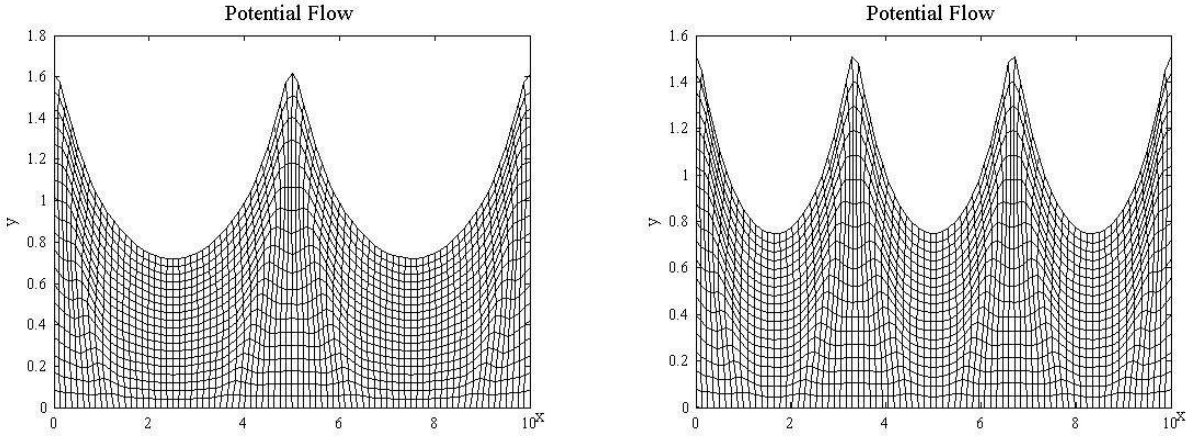

Figure 2: Wave profiles and grids for the test case of standing waves. To the left - the wavenumber is equal to 4, to the right - the wavenumber is equal to 6.

Evolution in time of wave profiles and velocity potentials are shown below at Fig. 3. The test case is standing waves with wave number 6.

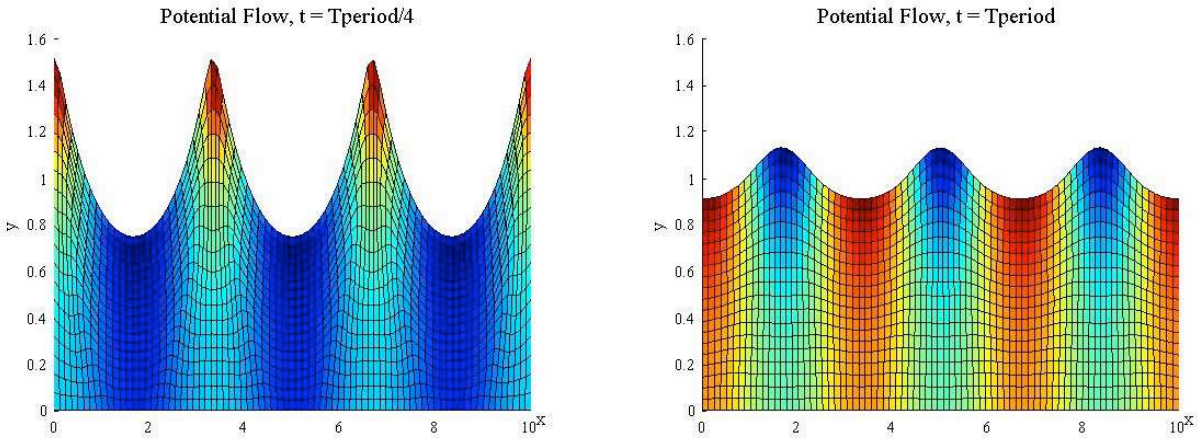

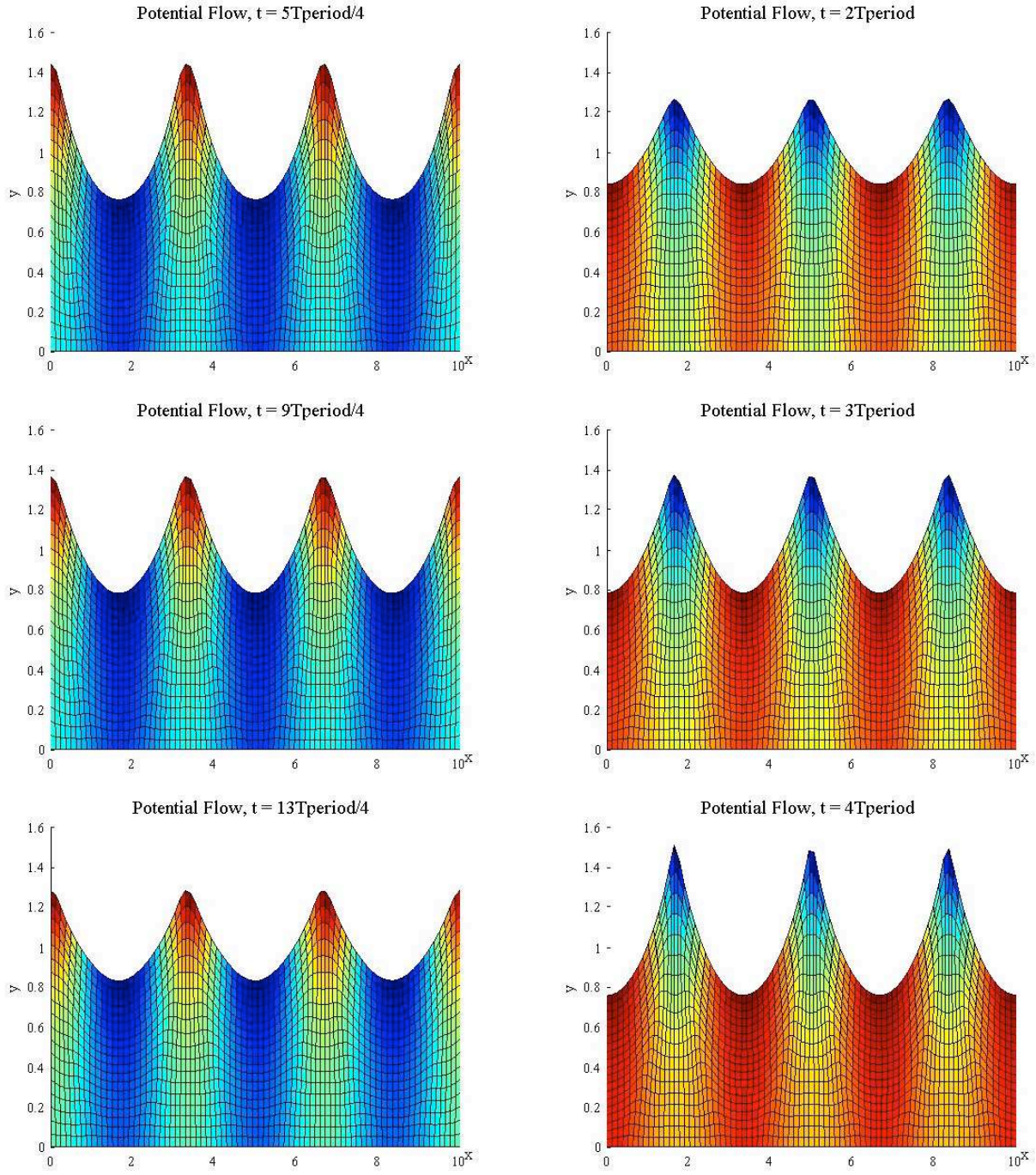

Figure 3: Wave profiles, corresponding grids and velocity potential fields for the test case of standing waves with wave number equal to 6. Various times are shown.

The variations in interior coordinates are connected to the variations of the free surface function through Knupp' equations (21) which allows the evaluation of Eq. (18). Therefore, the adaptive mesh movement is a part of the variational structure and this method is energy-conserving. The difference between initial energy and calculated energy oscillates between fixed boundaries as shown at Fig. 4 for 20 time periods.

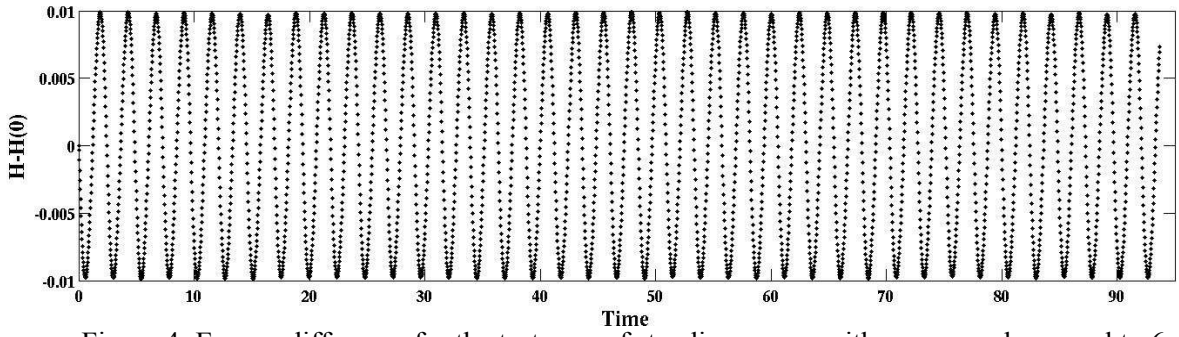

Figure 4: Energy difference for the test case of standing waves with wave number equal to 6.

5. Discussion and future plans

A systematic derivation of a new Hamiltonian formulation was given starting from the variational principle (1). Subsequently, we showed how that formulation could be reduced to the two limiting systems, and discussed how it is related to a Boussinesq model of Klopman et al (2010). A compatible, variational finite element discretization of Miles' variational principle was given as an intermediate step, including variational mesh movement. Simulations for nonlinear surface gravity waves on a moving mesh were presented. Immediate future plans include the implementation of a discretization of Luke's variational principle, since we can then capture wave overturning in the vertical plane. Subsequently, we will include bores into the numerical model based on a geometric analysis inspired by that proposed in Whitham (1974), but limited here to the vertical plane, such that the multivalued free surface is either only present at isolated points in the horizontal or is limited to exist numerically only in narrow strips around such points. The medium-term future plan involves full three-dimensional implementation and validation of the new water wave model.

References

Ambati, V.R., van der Vegt, J.J.W. and Bokhove, O. (2012) Variational Galerkin Finite Element Method for Nonlinear Water Waves. *In preparation*.

Cotter, C.J., Bokhove, O. (2010) Variational water-wave model with accurate dispersion and vertical vorticity. *J. Eng. Math*. 67, 33-54.

Klopman, G., van Groesen, B., Dingemans, M.W. (2010) A variational approach to Boussinesq modelling of fully nonlinear water waves. *J. Fluid Mech.* 657, 36-63.

Knupp, P.M. (1992) A robust elliptic grid generator. *J. Comp. Phys.* 100, 409-418.

Luke, J.C. (1967) A variational principle for a fluid with a free surface. *J. Fluid Mech.* 27, 395-397.

Miles, J. (1977) On Hamilton's principle for surface waves. *J. Fluid Mech.* 83, 153-158.

Peregrine, D.H. (1998) Surf zone currents. *Theor. Comput. Fluid Dyn.* 10, 295-310.

Peregrine, D.H., Bokhove O. (1998) Vorticity and Surf Zone Currents. *Proc. 26th Int. Conf. on Coastal Engineering 1998, ASCE, Copenhagen*, 745-758.

Salmon, R. (1988) Hamiltonian Fluid Mechanics. *Ann. Rev. Fluid Mech.* 20, 225-256.

Whitham, G.B. (1974) Linear and Nonlinear Waves. *New York: Wiley*, 635 pp.